TECHNICAL POINT OF VIEW

Cardiac Time-of-flight PET for Evaluating Myocardial Perfusion with ^{13}N-ammonia: Phantom Studies for Estimation of Defect and Heterogeneity

Shinro Matsuo, MD, PhD[1], Takafumi Mochizuki, MD, PhD[2], Satoru Takeda[2], Takayuki Shibutani, RT, MHSc[3], Masahisa Onoguchi, PhD[3], Kenichi Nakajima, MD, PhD[1], Koichi Okuda, PhD[4], Hirotoshi Takeuchi[2], Kazuya Hayakawa[2] and Seigo Kinuya, MD, PhD[1]

Received: May 26, 2016/Revised manuscript received: July 13, 2016/Accepted: July 14, 2016

Abstract

***Background*: Cardiac ^{13}N-ammonia (^{13}N-NH_3) positron emission tomography (PET) is approved by Japanese Ministry of Health, Labour and Welfare for diagnosis of ischemic heart disease. New PET camera recently has three-dimensional mode acquisition and ordered subset expectation maximization (OSEM) reconstruction with time-of-flight (TOF) and point spread function (PSF) correction technology. The aim of the phantom study was to evaluate the usefulness of this novel technology using ^{13}N-NH_3 and ^{18}F-fluorodeoxyglucose (^{18}F-FDG).**

***Method*: PET imaging was performed using a lung-heart torso phantom with myocardial perfusion defects. The indices of defect contrast, the coefficient of variation (CV) and the index of homogeneity were analyzed by using four reconstruction schemes, including OSEM, OSEM+TOF, OSEM+PSF, and TOF+PSF correction methods.**

***Results*: The phantom study showed that TOF resulted in improvements of defect lesion detectability with low statistical noise. The defect contrast index of TOF+PSF was significantly larger than that of OSEM only ($p=0.048$). The cardiac percent root mean square uncertainty (RMSU) with PSF was 25.9% in OSEM+PSF and 20.9 % in TOF+PSF. In contrast cardiac % RMSU without PSF correction was 14.8% in OSEM and 15.3% in TOF, which was lower than that with PSF correction. The average wall counts were homogeneous in four reconstruction methods in ^{13}N-NH_3. The value of % CV on the profile curve of ^{13}N-NH_3 images was confirmed to be smaller than 5% in all reconstruction methods.**

***Conclusions*: The new PET technology with TOF and PSF correction may extend the possibility of precise analysis of abnormal perfusion defects, and clinical applications are expected.**

Keywords: ^{13}N-ammonia, ^{18}F-fluorodeoxyglucose, Homogeneity, Point spread function correction, Time of flight

Ann Nucl Cardiol 2016；2（1）：73-78

As well as conventional single-photon-emission computed tomography (SPECT) approaches, Japanese Circulation Society guidelines address clinical indication for positron emission tomography (PET) (1). In Japan, ^{13}N-ammonia (^{13}N-NH_3) PET is reimbursed by Japanese Ministry of Health, Labour, and Welfare for diagnosis of ischemic heart disease when other tests are not able to make diagnosis (2). The dynamic acquisition capacity of myocardial perfusion imaging with PET may allow for absolute quantitative assessments and available for its higher accuracy in detecting flow-limiting coronary artery narrowing with more improved temporal and special resolution compared to conventional SPECT (3).

doi：10.17996/ANC.02.01.73

1) Shinro Matsuo, Kenichi Nakajima, Seigo Kinuya
Department of Nuclear Medicine, Kanazawa University Hospital, 13-1 Takara-machi, Kanazawa, Ishikawa, Japan 920-8641
E-mail: smatsuo@nmd.m.kanazawa-u.ac.jp
2) Takafumi Mochizuki, Satoru Takeda, Hirotoshi Takeuchi, Kazuya Hayakawa
PET Center, Kanazawa Advanced Medical Center, Ishikawa, Japan
3) Takayuki Shibutani, Masahisa Onoguchi
Department of Quantum Medical Technology, Institute of Medical Pharmaceutical and Health Science, Kanazawa University, Japan
4) Koichi Okuda
Department of Physics, Kanazawa Medical University, Ishikawa, Japan

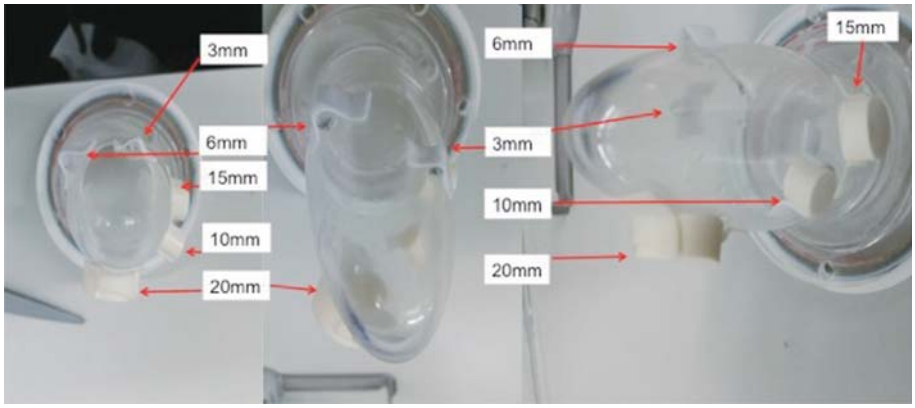

Fig. 1 Cardiac LH phantom: The myocardium has 5 perfusion defects, 3, 6, 10, 15 and 20mm in diameter.

Recently new time-of-flight (TOF) PET camera has become available. More quantitative patient data will be beneficial for clinical diagnosis of coronary artery disease.

Reconstruction is an essential step in the processing of cardiac PET imaging. Commonly used reconstruction algorithms for PET are filtered back projection (FBP) and ordered subsets expectation maximization (OSEM) methods (4). New PET cameras recently have three-dimensional (3D) mode acquisition and OSEM reconstruction with TOF and point spread function (PSF) correction technology. In clinical setting, patients' prognosis is often strongly related with the amount of perfusion defects (5,6). However there is few basic technical data on this new technology regarding defect detectability and image quality using ^{13}N-NH_3 cardiac PET. Therefore, the purpose of this phantom study was to elucidate the effect of OSEM reconstruction, to assess the effects of TOF and PSF on the estimation of myocardial perfusion abnormalities.

Material and methods

Data acquisition

A commercially available lung-heart torso phantom (Kyoto Kagaku Co., LTD, Kyoto, Japan) mimicking the shape of a heart was used for all acquisitions (Fig. 1). The phantom was developed to reduce a difference of image quality among institutions. The appearance and myocardial region of the phantom are shown in Fig. 1. This phantom was a model in which 5 perfusion defects were set and included the left ventricular cavity and my ocardium in the heart. The phantom could simulate and acquire 5 different defects simultaneously, namely the defects of 3, 6, 10, 15 and 20 mm in diameter. In this phantom, the defect area represented a scar, whereas the area without defect represented a viable myocardium. For all the acquisitions, the phantom was always placed at the same position on the bed of the PET/CT scanner.

^{13}N-NH_3 was generated using PET radiotracer production system called UG-M1 system (UNIVERSAL GIKEN CO., LTD, Kanagawa, Japan). The phantom was filled with ^{13}N-NH_3 with the myocardium-to-background ratio of 20. The concentration of ^{13}N-NH_3 solution was 40 kBq/ml and 2 kBq/ml for the left ventricular wall and cavity, respectively. ^{18}F-fluorodeoxyglucose (FDG) solution, to simulate clinical study, was administered into left ventricular wall (40 kBq/ml) and cavity (2 kBq/ml). All left ventricular spheres were filled with hot solution, while mediastinum and lung did not contain any radioisotope. Images were acquired in three dimensions (3D). All data were obtained with an Advance PET/CT scanner Discovery 690 (GE Healthcare Japan, Tokyo, Japan), a fully 3D TOF-PET scanner combined with a 16-slice CT scanner.

Reconstruction

Four reconstruction schemes were considered. The images were reconstructed with OSEM, OSEM+TOF, OSEM+PSF, and TOF+PSF correction methods in ^{13}N-NH_3. ^{18}F-FDG was used to image the phantom in the same manner of ^{13}N-NH_3. PET images were reconstructed by OSEM with 24 subsets and 6 iterations using the advanced workstation (AW) ver. 4.5, which incorporated attenuation and scatter corrections using the acquired computed tomography (CT) map of the phantom.

Post-reconstruction and image analysis

To investigate the basic property of the images in each reconstruction, visual and quantitative analysis was performed. The image quality was assessed by PET image with four reconstruction schemes, including OSEM, OSEM+TOF, OSEM+PSF and TOF+PSF correction methods. The scoring was made by mutual consent of nuclear medicine physicians (1, poor; 2, good).

After being reconstructed into short-axis images, region of interest (ROI) was placed on the myocardium (ROI 1) and on the defect (ROI 2) as shown in Fig. 2. The defect contrast indices were measured on each defect (6, 10, 15 and 20 in diameter) in four reconstruction methods, including OSEM,

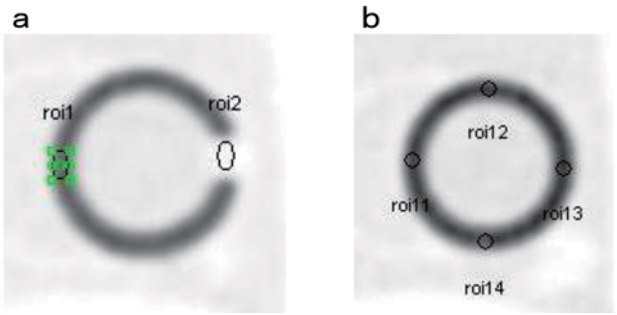

Fig. 2 Regions of interest were placed on the myocardium (ROI 1 =a) and on the 20mm defect (ROI 2=b), as shown in Fig. 2a. Defect contrast index was defined as (a-b)/(a+b). Four ROIs of the same size to the spheres were drawn in the septal (ROI 11), anterior (ROI 12), lateral (ROI 13) and inferior (ROI 14) walls of the myocardium (Fig. 2b).

OSEM + TOF, OSEM + PSF, and TOF + PSF correction methods. The average values were measured and defined as "a" in the ROI 1, and as "b" in the ROI 2. The defect contrast index was defined by the formula: (a-b)/(a+b). The profile curves using short-axis images were created to measure the uptake of the perfusion defect of the left ventricle.

Four circular ROIs of the same size were drawn in the septal, anterior, lateral and inferior walls on the mid-ventricular short-axis slice (Fig. 2). Average count and standard deviation were obtained from the count of the ROI. The percent root mean square uncertainty (% RMSU) reflecting the image noise was given by the following equation: % RMSU = standard deviation /average count ×100% (7,8). Average count on each wall was calculated to see homogeneity of wall count.

From the profile curve using short-axis images in normal myocardium, the count of pixels was calculated per 6 degrees from the center of the image, and % coefficient of variation (CV) was determined.

The study was approved by the institutional review board (IRB).

Statistical analysis

Data were expressed as mean ± standard deviation (SD). Statistical analysis was performed using JMP 10.0.2 (SAS Institute Inc., Cary, NC, USA). A student t-test was applied to compare the values of two groups. A p value of <0.05 was considered as statistically significant.

Results

The reconstructed short-axis images were shown in Fig. 3. Visual analysis showed that all PET images were considered to be good and clinically applicable with score 2. Expert visual evaluation for the comparison between ^{13}N-NH_3 and ^{18}F-FDG suggested that the PET images of ^{18}F-FDG were identical in image quality to that of ^{13}N-NH_3. In comparison with OSEM images, defects with a diameter of 3, 6, 10, 15 and 20 mm in TOF and PSF images showed clear edge on visual evaluation. In ^{13}N-NH_3 PET image showed that the reconstructed images with TOF had clearer edges of the left ventricular wall compared to that without TOF. Moreover the decreased activity of ^{13}N-NH_3 was more noticeable in the images with TOF and PSF. ^{18}F-FDG images also showed that smaller partial volume effect with higher image contrast with TOF acquisition compared to that without TOF (Fig. 3). A tiny non-transmural myocardial perfusion defect in 3mm diameter could be recognized with high visual image quality of PET with TOF and PSF technology. The novel PET cameras with TOF and PSF made it possible to observe small sized defects (Fig. 3).

Quantitative analysis

Fig. 4 shows four types of reconstructed slice through the myocardial defect and profile curves were obtained from the ^{13}N- NH_3 PET image. The profile curves of ^{18}F-FDG are illustrated in Fig. 5. For both ^{13}N-NH_3 and ^{18}F-FDG PET imeges, better defect contrast was observed in OSEM+PSF, and TOF+PSF, while the noise was smaller in OSEM and TOF. Horizontal and vertical profile curves obtained in different reconstruction methods are illustrated in Fig. 6. The profile curves reconstructed with PSF were sharp and high compared to those without PSF.

The defect contrast indices of ^{13}N-NH_3 when reconstructed with TOF+PSF was the highest and the best (0.65 ± 0.07) among the four methods. The defect contrast indices of ^{13}N-NH_3 were 0.54 ± 0.04 when reconstructed with OSEM, 0.55 ± 0.11 in TOF, 0.64 ± 0.08 in OSEM+PSF. The defect contrast indices of TOF+PSF was significantly higher than that of OSEM ($p=0.048$). The defect contrast indices of ^{18}F-FDG were 0.59 ± 0.1 in OSEM, 0.59 ± 0.09 in TOF, 0.69 ± 0.1 in OSEM+PSF, and 0.68 ± 0.08 in TOF+PSF. The defect contrast indices tended to be higher in that of TOF+PSF compared to that of OSEM both in ^{13}N-NH_3 and in ^{18}F-FDG.

The cardiac % RMSU among septal, anterior, lateral and inferior walls using ^{13}N-NH_3, when reconstructed with PSF, was 25.9% in OSEM+PSF and 20.9% in TOF+PSF. The cardiac % RMSU without PSF was 14.8% in OSEM and 15.3 % in TOF. The cardiac % RMSU using ^{18}F-FDG, when reconstructed with PSF was 20.3% in OSEM+PSF and 21.4% in TOF+PSF. The cardiac % RSMU without PSF was 17.3% in OSEM and 15.4% in TOF. The average counts in four walls were homogeneous in all four reconstruction methods in ^{13}N-NH_3 and ^{18}F-FDG.

The values of % CV of both ^{13}N-NH_3 and ^{18}F-FDG were confirmed smaller than 5% in all reconstruction methods. The % CV in walls without defects using ^{13}N-NH_3 was 3.9% when reconstructed with OSEM. The % CV was 4.8% in TOF, 4.2%

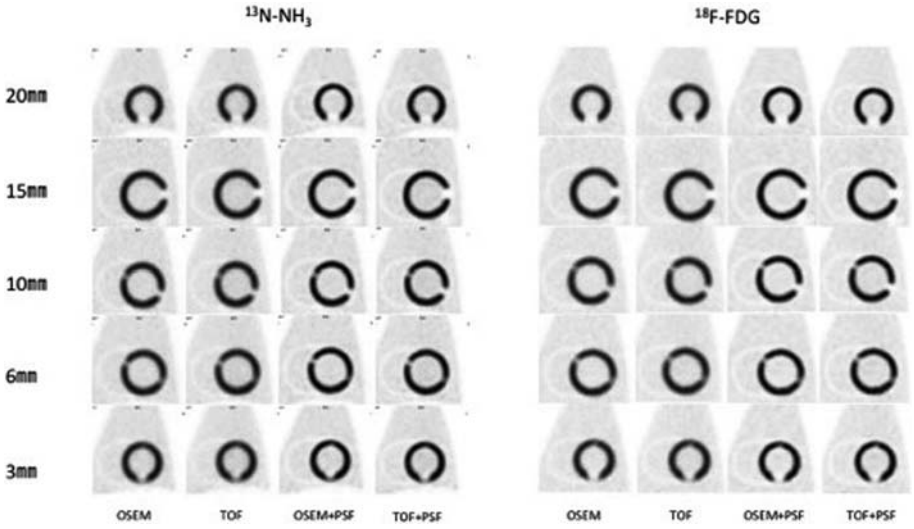

Fig. 3　Short-axis SPECT images with a perfusion defect
The images were reconstructed with OSEM, TOF, OSEM+PSF, and TOF+PSF in ^{13}N-NH_3 and ^{18}F-FDG.
OSEM: ordered subsets expectation maximization; TOF: time-of-flight; PSF: point spread function.

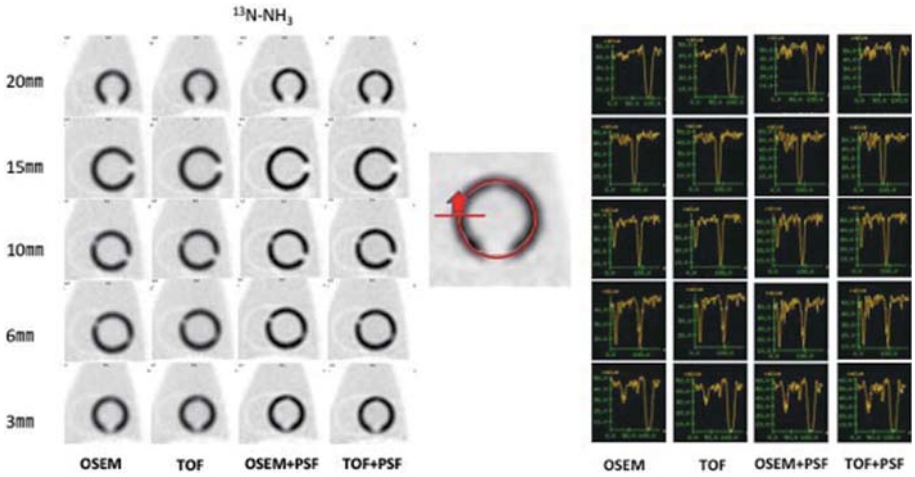

Fig. 4　Phantom images and profile curve in each reconstruction in ^{13}N-NH_3
The images were reconstructed with OSEM, TOF, OSEM+PSF and TOF+PSF in ^{13}N-NH_3 and ^{18}F-FDG. A starting point of the profile curve is shown with the red arrow, creating a curve in the clockwise.
OSEM: ordered subsets expectation maximization; TOF: time-of-flight; PSF: point spread function.

in OSEM+PSF and 4.3% in TOF+PSF. The % CV in walls without defects using ^{18}F-FDG was 4.6% when reconstructed with OSEM. The % CV was 4.9% in TOF, 4.1% in OSEM+PSF and 4.7% in TOF+PSF.

Discussion

This study directly compared the PET images for the estimation of defect using cardiac phantom with simulated infarcts. This phantom experiment showed that novel PET imaging with TOF and PSF correction method had a better image compared to that of conventional PET. The results obtained from this phantom study are quite consistent with previous reports and quite reasonable on the basis of TOF concept (9,10).

Few PET data are available about the quantification of myocardial defect size using cardiac phantoms. Matsunari et al. reported ^{18}F-labeled agent could accurately measure the defect size (11). In recent PET study, PSF modeling is an effective approach to increase corrections between neighboring voxels. Recently, Slomka et al. reported PMOD software has a high reproducibility of the quantitative analysis using ^{13}N- NH^3 myocardial PET study (10). ^{13}N-NH_3 TOF PET imaging has reportedly better reproducibility of intra- and inter-observer variation compared to non-TOF (4). The measurement of coronary flow reserve also achieved high reproducibility using TOF acquisition technique (12). More

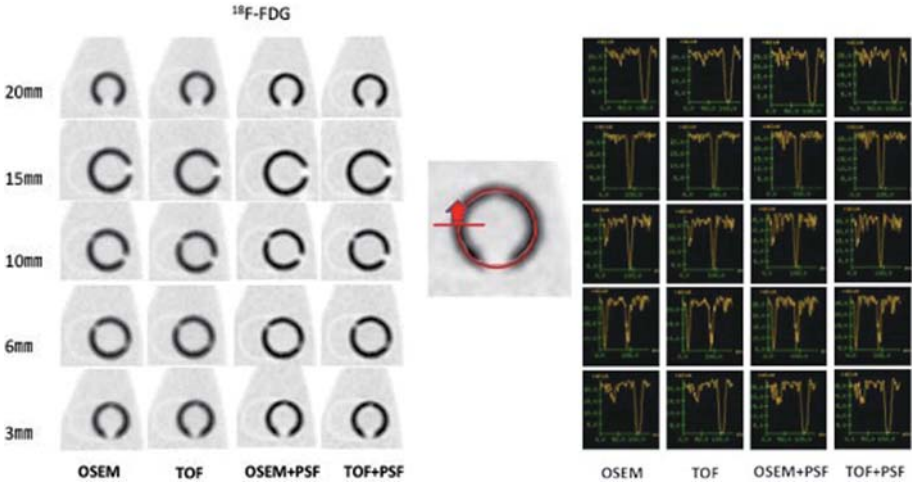

Fig. 5 Phantom images and profile curve in each reconstruction in ^{18}F-FDG
The images were reconstructed with OSEM, TOF, OSEM+PSF and TOF+PSF in ^{18}F-FDG. A starting point of the profile curve is shown with the red arrow, creating a curve in the clockwise.
OSEM: ordered subsets expectation maximization; TOF: time-of-flight; PSF: point spread function.

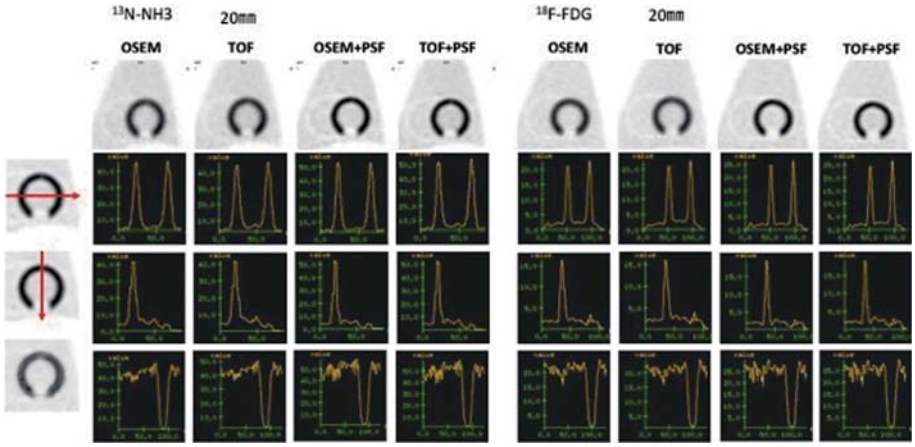

Fig. 6 Phantom images and profile curve obtained in each reconstruction
The profile curves reconstructed with PSF are sharp and high.
OSEM: ordered subsets expectation maximization; TOF: time-of-flight; PSF: point spread function.

recent report showed that PET/CT images allowed a significant misregistration-artifactual reduction in ^{13}N-NH_3 tracer uptake in heart regions overlapping lung, when images were reconstructed with 3D ordered-subset expectation maximization combined with TOF and PSF (13). TOF-PET uses the difference between the arrival times of coincident photons to estimate the location of the annihilation of the positron. The PSF modeling might be used in cardiac fields to minimize the noise at a given noise level. In accordance with previous studies (4,10), this phantom study demonstrated that PET imaging with novel technology, including TOF and PSF, improved greatly the image quality and decreased noise in cardiac perfusion examinations. The key advantage of advanced quantitative analysis with TOF leads to the improved reproducibility and reduced intra-observer variability (4). The assessment of myocardial homogeneity might depend on the noise.

Visual analysis in this study showed good inter-observer agreement. Quantative analysis including visual analysis, uptake, mean count, standard deviation, defect contrast, % RSMU, % CV were also applied for an objective assessment. The results of this study elucidated improved homogeneity of myocardial tracer distribution by TOF PET compared to non-TOF PET. Our results confirmed better image quality and homogeneity when TOF and PSF were applied. The value of % CV of ^{13}N-NH_3 was confirmed smaller than 5%, which indicated homogenous counts in all myocardial walls. Visualization of a myocardial defect depends on the noise level and the contrast between the defects and surrounding myocardium. Our study showed that an accurate identification of the myocardial defect could become possible by using TOF and PSF correction technology (14,15). This phantom study

showed excellent images in ^{13}N-NH_3 as well as ^{18}F-FDG. The homogeneity of ^{13}N-NH_3 PET image was comparable to that of ^{18}F-FDG image.

There are some limitations in this study. Firstly we did not evaluate the defects and ischemia as a dynamic flow measurement in clinical studies. Secondly we did not use Compton scatter correction, which might be useful in the future PET imaging (16,17). In clinical applications, further investigation is needed to clarify the influence of the tracer difference on image quality and influx rate constants of the tracers (18).

Conclusion

The new PET/CT camera employing 3D PET/CT with 3D OSEM, TOF and PSF algorithms broadened the possibility of precise analysis of abnormal perfusion. The novel ^{13}N-NH_3 myocardial PET using TOF and PSF information might have the potential for better quantification of the absolute value of myocardial flow. Both diagnostic and prognostic studies using new technology should be performed with many patients of coronary artery disease.

Acknowledgments

This study was supported by JSPS Grants-in-Aid for Scientific Research (C) in Japan (Grant Number 23591755, PI Shinro Matsuo).

Sources of funding

None

Conflicts of interest

None

Reprint requests and correspondence:
Shinro Matsuo, MD, PhD
Department of Nuclear Medicine, Kanazawa University Hospital, 13-1 Takara-machi, Kanazawa, Ishikawa, Japan 920-8641
E-mail: smatsuo@nmd.m.kanazawa-u.ac.jp

References

1. Tamaki N. Guidelines for clinical use of cardiac nuclear medicine (JCS 2010) -digest version. Circ J 2012; 76: 761-7.
2. Yoshinaga K. Current Japanese ministry of health, labor, and welfare approval of cardiac positron emission tomography. Ann Nucl Cardiol 2015; 1(1): 106-7.
3. Yoshinaga K, Tomiyama Y, Suzuki E, et al. Myocardial blood flow quantification using positron emission tomography. Circ J 2013; 77: 1662-71.
4. Suga M, Onoguchi M, Tomiyama T, et al. The reproducibility of time-of-flight PET and conventional PET for quantification of myocardial blood flow and coronary flow reserve with ^{13}N-ammonia. J Nucl Cardiol 2016; 23: 457-72.
5. Nishimura T, Nakajima K, Kusuoka H, et al. Prognostic study of risk stratification among Japanese patients with ischemic heart disease using gated myocardial perfusion SPECT: J-ACCESS study. Eur J Nucl Med Mol Imaging 2008; 35: 319-28.
6. Matsuo S, Nakajima K, Horie M, et al. Prognostic value of normal stress myocardial perfusion imaging in Japanese population. Circ J 2008; 72: 611-7.
7. Kenda S, Onishi H, Nakamoto K. Optimization of reconstruction parameters using a multi-focus fan beam collimator in myocardial perfusion single photon emission computed tomography study. Nihon Hoshasen Gijutsu Gakkai Zasshi 2014; 70: 662-9.
8. Kita A, Onoguchi M, Sugimoto K, et al. Development of simple processing for deleting undershooting artifact using the FBP method — evaluation of simulation data —. Nihon Hoshasen Gijutsu Gakkai Zasshi. 2015; 71: 201-7.
9. Schaefferkoetter J, Ouyang J, Rakvongthai Y, et al. Effect of time-of-flight and point spread function modeling on detectability of myocardial defects in PET. Med Phys 2014; 41: 062502.
10. Slomka PJ, Berman DS, Germano G. New cardiac cameras: single-photon emission CT and PET. Semin Nucl Med 2014; 44: 232-51.
11. Matsunari I, Yoneyama T, Kanayama S, et al. Phantom studies for estimation of defect size on cardiac ^{18}F SPECT and PET: implications for myocardial viability assessment. J Nucl Med 2001; 42: 1579-85.
12. Schindler TH, Quercioli A, Valenta I, et al. Quantitative assessment of myocardial blood flow. Clinical and research applications. Semin Nucl Med 2014; 44: 274-93.
13. Tomita Y, Ishida M, Ichikawa Y, et al. The effect of misregistration between CT-attenuation and PET-emission images in ^{13}N-ammmonia myocardial PET/CT. J Nucl Med Technol 2016; 44: 73-7.
14. Surti S, Karp J. Experimental evaluation of a simple lesion detection task with time-of-flight PET. Phys Med Biol 2009; 54: 373-84.
15. Karp JS, Surti S, Daube-Witherspoon M, et al. Benefit of time-of-flight in PET: Experimental and clinical results. J Nucl Med 2008; 49: 462-70.
16. Matsuo S, Nakajima K, Okuda K, et al. Standardization of the heart-to-mediastinum ratio of ^{123}I-labelled-metaiodobenzylguanidine uptake using the dual energy window method: feasibility of correction with different camera-collimator combinations. Eur J Nucl Med Mol Imaging 2009; 36: 560-6.
17. Levin CS, Dahlbom M, Hoffman EJ. A Monte Carlo correction for the effect of Compton scattering in 3-D PET brain imaging. IEEE Transactions on Nuclear Science 1995; 42: 1181-5.
18. Kudo T, Hata T, Kagawa S, et al. Simple quantification of myocardial perfusion by pixel-by-pixel graphical analysis using carbon-11 acetate: comparison of the K-complexes of carbon-11 acetate and nitrogen-13 ammonia. Nucl Med Commun 2008; 29: 679-85.